Journal of the Optical Society of America B
OPTICAL PHYSICS

Strong circular dichroism of core-shell magnetoplasmonic nanoparticles

PARIS VARYTIS,[1,*] NIKOLAOS STEFANOU,[1] ARISTI CHRISTOFI,[2] AND NIKOLAOS PAPANIKOLAOU[2]

[1]Department of Solid State Physics, National and Kapodistrian University of Athens, University Campus, GR-157 84 Athens, Greece
[2]Institute of Nanoscience and Nanotechnology, NCSR "Demokritos," GR-153 10 Athens, Greece
*Corresponding author: parisvarytis@phys.uoa.gr

Received 26 March 2015; revised 2 April 2015; accepted 3 April 2015; posted 9 April 2015 (Doc. ID 237027); published 8 May 2015

Composite magnetoplasmonic nanoparticles with a core-shell morphology exhibit intriguing optical properties and offer impressive opportunities for tailoring in a controllable manner the light-matter interaction at subwavelength dimensions. These properties are usually analyzed in the framework of the quasi-static approximation, which, however, is often inadequate; thus, a full electrodynamic treatment is required. In this respect, we developed a rigorous method for an accurate description of electromagnetic scattering by a gyrotropic sphere coated with a nongyrotropic concentric spherical shell, based on the full multipole expansion of the wave field. The method was applied to specific examples of core-shell cobalt-silver spherical nanoparticles, where the occurrence of strong circular dichroism induced by magnetoplasmonic interaction, which largely exceeds that of homogeneous noble metal nanoparticles in an external magnetic field, was found. Our results were also explained by reference to the quasi-static approximation, which, though it reproduces the main features of the absorption spectra, strongly overestimates circular dichroism in the cases we studied.

OCIS codes: (050.1930) Dichroism; (160.3820) Magneto-optical materials; (160.4236) Nanomaterials; (250.5403) Plasmonics; (290.4020) Mie theory.

http://dx.doi.org/10.1364/JOSAB.32.001063

1. INTRODUCTION

Particle plasmons refer to localized modes of the electromagnetic (EM) field, e.g., in a noble metal nanoparticle, which are able to confine light in subwavelength volumes and achieve huge local field enhancement at specific frequencies that can be tuned within a relatively broad spectrum by changing the particle species, size, shape, and/or its environment [1]. All of these properties render particle plasmons suitable for enhancing the light-matter interaction and developing nanophotonic devices, sensing, light-harvesting applications, etc.

Controlling particle plasmons with a magnetic field provides further opportunities for designing active plasmonic components. In this context, it has been shown that 3D chiral structures and surfaces of crystals of plasma spheres in an external static uniform magnetic field that lack, simultaneously, time-reversal and space-inversion symmetries exhibit a nonreciprocal spectral response [2,3], which is a key issue in the development of nonreciprocal photonic devices. Moreover, it has been reported that magnetoplasmonic modes observed on colloidal gold nanoparticles by means of magnetic circular dichroism spectroscopy could be useful for detecting changes in the refractive index of the surrounding medium and, thus, developing refractometric sensing applications [4]. However, though noble metals, like gold and silver, are excellent plasmonic materials, they show very weak magneto-optical activity at moderate magnetic fields. On the other hand, ferromagnetic metals that exhibit strong magneto-optical effects lack competitive plasmonic properties due to high optical losses. In this respect, combining ferromagnets with noble metals opens new routes in the development of efficient and versatile magnetoplasmonic architectures [5]. For example, strong enhancement of the magneto-optical Faraday rotation has been observed in all-metal core-shell cobalt-silver nanoparticles due to localized surface plasmon resonance [6].

For a rigorous theoretical description of the optical response of composite core-shell magnetoplasmonic particles, beyond the quasi-static approximation, a full electrodynamic method is clearly needed. In the present paper, we develop such a method following the Mie approach to the scattering problem, which is based on the multipole expansion of the EM field in the gyrotropic core, isotropic shell, and host regions and, subsequently, proper matching of the wave field at the interfaces. The applicability of the method is demonstrated in specific examples of core-shell cobalt-silver nanospheres, where evidence for the occurrence of strong circular dichroism is provided.

2. THEORETICAL METHOD

Material gyrotropy at optical and infrared frequencies is usually described by a relative permittivity tensor,

$$\overleftrightarrow{\epsilon}_g = \epsilon_z \begin{pmatrix} \epsilon_r & -i\epsilon_\kappa & 0 \\ i\epsilon_\kappa & \epsilon_r & 0 \\ 0 & 0 & 1 \end{pmatrix}, \tag{1}$$

if we take the gyration vector along the z axis and a scalar relative permeability μ_g. Starting from Maxwell equations for the spatial part of a monochromatic EM field of angular frequency ω with $\exp(-i\omega t)$ time dependence inside such a sourceless medium: $\nabla \cdot \mathbf{B}(\mathbf{r}) = 0$, $\nabla \cdot \mathbf{D}(\mathbf{r}) = 0$, $\nabla \times \mathbf{E}(\mathbf{r}) = i\omega \mathbf{B}(\mathbf{r})$, and $\nabla \times \mathbf{H}(\mathbf{r}) = -i\omega \mathbf{D}(\mathbf{r})$ and the constitutive relations $\mathbf{B}(\mathbf{r}) = \mu_0 \mu_g \mathbf{H}(\mathbf{r})$ and $\mathbf{D}(\mathbf{r}) = \epsilon_0 \overleftrightarrow{\epsilon}_g \mathbf{E}(\mathbf{r})$, we obtain the wave equation

$$\nabla \times \nabla \times [\epsilon_z \overleftrightarrow{\epsilon}_g^{-1} \mathbf{D}(\mathbf{r})] - q_g^2 \mathbf{D}(\mathbf{r}) = 0, \tag{2}$$

with $q_g^2 = \omega^2 \epsilon_z \mu_g \epsilon_0 \mu_0 = \epsilon_z \mu_g \omega^2 / c^2$.

Following the approach of Lin and Chui [7], we solve Eq. (2) by expanding the wave field into the specific vector-spherical-wave basis employed in our layer-multiple-scattering method [8,9]. For this purpose, we define a set of longitudinal (irrotational) spherical wave functions corresponding to a wavenumber q as

$$\begin{aligned} &\mathbf{F}_{Llm}(q, \mathbf{r}) = \frac{1}{q} \nabla [f_l(qr) Y_{lm}(\hat{\mathbf{r}})], \\ &l = 0, 1, 2, \ldots; m = -l, -l+1, \ldots, l, \end{aligned} \tag{3}$$

where Y_{lm} are the usual spherical harmonics and f_l may be any linear combination of the spherical Bessel function, j_l, and the spherical Hankel function, h_l^+. Similarly, we consider a set of transverse (divergenceless) spherical wave functions given by

$$\begin{aligned} \mathbf{F}_{Hlm}(q, \mathbf{r}) &= f_l(qr) \mathbf{X}_{lm}(\hat{\mathbf{r}}), \\ \mathbf{F}_{Elm}(q, \mathbf{r}) &= \frac{i}{q} \nabla \times [f_l(qr)\, \mathbf{X}_{lm}(\hat{\mathbf{r}})], \\ &l = 1, 2, \ldots; m = -l, -l+1, \ldots, l, \end{aligned} \tag{4}$$

where $\mathbf{X}_{lm}$ are the vector spherical harmonics. The above vector spherical wave functions constitute a complete basis set for the expansion of any vector field in the sense of Helmholtz theorem [10].

The divergenceless property, $\nabla \cdot \mathbf{D}(\mathbf{r}) = 0$, implies that $\mathbf{D}$ can be expanded in terms of $\mathbf{F}_{Hlm}$ and $\mathbf{F}_{Elm}$, and it does not involve $\mathbf{F}_{Llm}$, as follows:

$$\begin{aligned} \mathbf{D}(\mathbf{r}) = \sum_j b_j \frac{q_j^2}{q_g^2} \epsilon_0 \epsilon_z \sum_{lm} [&a_{Hlm;j} \mathbf{F}_{Hlm}(q_j, \mathbf{r}) \\ &+ a_{Elm;j} \mathbf{F}_{Elm}(q_j, \mathbf{r})], \end{aligned} \tag{5}$$

where b_j are expansion coefficients that can be determined from the appropriate boundary conditions, while the wavenumbers q_j and the associated spherical-wave amplitudes $a_{Plm;j}$, with $P = H, E$, are obtained from the solution of the following eigenvalue equation [11]:

$$\sum_{P'=H,E} \sum_{l'm'} A_{Plm;P'l'm'} a_{P'l'm';j} = \frac{q_g^2}{q_j^2} a_{Plm;j}, \tag{6}$$

where the subscript $j = 1, 2, \ldots$ enumerates the eigenvalues and eigenvectors of the matrix $\mathbf{A}$. Explicit expressions for the matrix elements of $\mathbf{A}$ are provided in the appendix. With $\mathbf{D}$ given by Eq. (5), it follows from the equation $i\omega\mu_0\mu_g \mathbf{H}(\mathbf{r}) = \nabla \times \mathbf{E}(\mathbf{r})$ and from the constitutive relations that the corresponding electric and magnetic field components have the form

$$\begin{aligned} \mathbf{E}(\mathbf{r}) = \sum_j b_j \sum_{lm} \Bigg[&\frac{q_j^2}{q_g^2} w_{lm;j} \mathbf{F}_{Llm}(q_j, \mathbf{r}) + a_{Hlm;j} \mathbf{F}_{Hlm}(q_j, \mathbf{r}) \\ &+ a_{Elm;j} \mathbf{F}_{Elm}(q_j, \mathbf{r}) \Bigg], \\ \mathbf{H}(\mathbf{r}) = \sum_j b_j \frac{q_j}{\omega \mu_0 \mu_g} \sum_{lm} [&a_{Elm;j} \mathbf{F}_{Hlm}(q_j, \mathbf{r}) \\ &- a_{Hlm;j} \mathbf{F}_{Elm}(q_j, \mathbf{r})], \end{aligned} \tag{7}$$

where explicit expressions for $w_{lm;j}$ are given in the appendix.

We now assume a homogeneous gyrotropic sphere coated with a concentric spherical shell of homogeneous and isotropic material characterized by scalar EM parameters ϵ_s and μ_s. The coated sphere, with outer radius S and inner radius S_c, is centered at the origin of coordinates in a homogeneous and isotropic host medium characterized by ϵ_h and μ_h and is illuminated by a plane EM wave of angular frequency ω. We write the EM field inside the gyrotropic spherical core according to Eqs. (3), (4), and (7) as

$$\begin{aligned} \mathbf{E}_c(\mathbf{r}) = \sum_j b_j \sum_{lm} \Bigg[&\frac{q_j^2}{q_g^2} w_{lm;j} \frac{1}{q_j} \nabla [j_l(q_j r) Y_{lm}(\hat{\mathbf{r}})] \\ &+ a_{Hlm;j} j_l(q_j r) \mathbf{X}_{lm}(\hat{\mathbf{r}}) \\ &+ a_{Elm;j} \frac{i}{q_j} \nabla \times j_l(q_j r) \mathbf{X}_{lm}(\hat{\mathbf{r}}) \Bigg] \\ \mathbf{H}_c(\mathbf{r}) = \sum_j b_j \frac{q_j}{\omega \mu_0 \mu_g} \sum_{lm} \Bigg[&a_{Elm;j} j_l(q_j r) \mathbf{X}_{lm}(\hat{\mathbf{r}}) \\ &- a_{Hlm;j} \frac{i}{q_j} \nabla \times j_l(q_j r) \mathbf{X}_{lm}(\hat{\mathbf{r}}) \Bigg], \end{aligned} \tag{8}$$

because the field must be finite everywhere, thus, only regular vector spherical waves that involve j_l enter in the expansion of Eq. (8). In the shell region, we express the EM field at the given frequency as a linear combination of the regular and irregular transverse vector spherical waves:

$$\mathbf{E}_s(\mathbf{r}) = \sum_{lm}\Big[a^{0s}_{Hlm} j_l(q_s r)\mathbf{X}_{lm}(\hat{\mathbf{r}}) + \frac{i}{q_s} a^{0s}_{Elm}\nabla\times j_l(q_s r)\mathbf{X}_{lm}(\hat{\mathbf{r}}) + a^{+s}_{Hlm} h^+_l(q_s r)\mathbf{X}_{lm}(\hat{\mathbf{r}}) + \frac{i}{q_s} a^{+s}_{Elm}\nabla\times h^+_l(q_s r)\mathbf{X}_{lm}(\hat{\mathbf{r}})\Big]$$

$$\mathbf{H}_s(\mathbf{r}) = \sqrt{\frac{\epsilon_s\epsilon_0}{\mu_s\mu_0}}\sum_{lm}\Big[a^{0s}_{Elm} j_l(q_s r)\mathbf{X}_{lm}(\hat{\mathbf{r}}) - \frac{i}{q_s} a^{0s}_{Hlm}\nabla\times j_l(q_s r)\mathbf{X}_{lm}(\hat{\mathbf{r}}) + a^{+s}_{Elm} h^+_l(q_s r)\mathbf{X}_{lm}(\hat{\mathbf{r}}) - \frac{i}{q_s} a^{+s}_{Hlm}\nabla\times h^+_l(q_s r)\mathbf{X}_{lm}(\hat{\mathbf{r}})\Big], \quad (9)$$

where $q_s = \omega\sqrt{\epsilon_s\mu_s}/c$ is the corresponding wavenumber and the coefficients a^{0s}_{Plm} and a^{+s}_{Plm} refer to the regular and irregular spherical waves, respectively. A similar expansion holds in the host region with an index h instead of s to denote the relevant quantities.

Applying the boundary conditions of continuity of the tangential components of the EM field at the core-shell interface, we can relate the coefficients of the irregular spherical waves in the shell region, a^{+s}_{Plm}, to those of the corresponding regular waves in the same region, a^{0s}_{Plm}, through the scattering T matrix of the spherical core embedded in the shell medium that, we assume, extends to infinity, which we denote here by T_c. In matrix form, we have

$$\mathbf{a}^{+s} = \mathbf{T}_c\mathbf{a}^{0s}, \quad (10)$$

where

$$\mathbf{T}_c = (\mathbf{\Lambda} - \mathbf{\Lambda}')^{-1}(\mathbf{V} - \mathbf{U})(\mathbf{U} + \mathbf{\Lambda}\mathbf{Z})^{-1}, \quad (11)$$

with

$$\Lambda_{Plm;P'l'm'} = -\frac{h^+_l(q_s S_c)}{j_l(q_s S_c)}\delta_{PP'}\delta_{ll'}\delta_{mm'},$$
$$\Lambda'_{Plm;P'l'm'} = -\frac{[x h^+_l(x)]'_{q_s S_c}}{[x j_l(x)]'_{q_s S_c}}\delta_{PP'}\delta_{ll'}\delta_{mm'}$$
$$U_{Hlm;j} = \frac{j_l(q_j S_c)}{j_l(q_s S_c)} a_{Hlm;j},$$
$$U_{Elm;j} = \frac{\mu_s q_j j_l(q_j S_c)}{\mu_g q_s j_l(q_s S_c)} a_{Elm;j}$$
$$V_{Hlm;j} = \frac{\mu_s [x j_l(x)]'_{q_j S_c}}{\mu_g [x j_l(x)]'_{q_s S_c}} a_{Hlm;j},$$
$$V_{Elm;j} = \frac{q_s [x j_l(x)]'_{q_j S_c}}{q_j [x j_l(x)]'_{q_s S_c}} a_{Elm;j} - \frac{\sqrt{l(l+1)}\, q_j q_s j_l(q_j S_c)}{q_g^2 [x j_l(x)]'_{q_s S_c}} w_{lm;j}. \quad (12)$$

The boundary conditions for the EM field at the shell-host interface lead to a system of linear equations, which can be written in matrix form as follows:

$$\mathbf{A}^{0h}\mathbf{a}^{0h} + \mathbf{A}^{+h}\mathbf{a}^{+h} = \mathbf{A}^{0s}\mathbf{a}^{0s} + \mathbf{A}^{+s}\mathbf{a}^{+s}$$
$$\mathbf{B}^{0h}\mathbf{a}^{0h} + \mathbf{B}^{+h}\mathbf{a}^{+h} = \mathbf{B}^{0s}\mathbf{a}^{0s} + \mathbf{B}^{+s}\mathbf{a}^{+s}, \quad (13)$$

where $\mathbf{A}^{0h}$, $\mathbf{A}^{+h}$, $\mathbf{A}^{0s}$, $\mathbf{A}^{+s}$, $\mathbf{B}^{0h}$, $\mathbf{B}^{+h}$, $\mathbf{B}^{0s}$, and $\mathbf{B}^{+s}$ are diagonal matrices with the following elements:

$$A^{0h}_{Hlm;Hlm} = j_l(q_h S), \qquad A^{0h}_{Elm;Elm} = \sqrt{\frac{\epsilon_h\mu_s}{\epsilon_s\mu_h}} j_l(q_h S),$$
$$A^{0s}_{Hlm;Hlm} = A^{0s}_{Elm;Elm} = j_l(q_s S),$$
$$A^{+h}_{Hlm;Hlm} = h^+_l(q_h S), \qquad A^{+h}_{Elm;Elm} = \sqrt{\frac{\epsilon_h\mu_s}{\epsilon_s\mu_h}} h^+_l(q_h S),$$
$$A^{+s}_{Hlm;Hlm} = A^{+s}_{Elm;Elm} = h^+_l(q_s S),$$
$$B^{0h}_{Hlm;Hlm} = \frac{\mu_s}{\mu_h}[x j_l(x)]'_{q_h S}, \qquad B^{0h}_{Elm;Elm} = \sqrt{\frac{\epsilon_s\mu_s}{\epsilon_h\mu_h}}[x j_l(x)]'_{q_h S},$$
$$B^{0s}_{Hlm;Hlm} = B^{0s}_{Elm;Elm} = [x j_l(x)]'_{q_s S},$$
$$B^{+h}_{Hlm;Hlm} = \frac{\mu_s}{\mu_h}[x h^+_l(x)]'_{q_h S}, \qquad B^{+h}_{Elm;Elm} = \sqrt{\frac{\epsilon_s\mu_s}{\epsilon_h\mu_h}}[x h^+_l(x)]'_{q_h S},$$
$$B^{+s}_{Hlm;Hlm} = B^{+s}_{Elm;Elm} = [x h^+_l(x)]'_{q_s S}. \quad (14)$$

Equations (10) and (13) can be solved to give

$$\mathbf{a}^{+h} = \mathbf{T}\mathbf{a}^{0h}, \quad (15)$$

where

$$\mathbf{T} = [(\mathbf{B}^{0s} + \mathbf{B}^{+s}\mathbf{T}_c)^{-1}\mathbf{B}^{+h} - (\mathbf{A}^{0s} + \mathbf{A}^{+s}\mathbf{T}_c)^{-1}\mathbf{A}^{+h}]^{-1} \times [(\mathbf{A}^{0s} + \mathbf{A}^{+s}\mathbf{T}_c)^{-1}\mathbf{A}^{0h} - (\mathbf{B}^{0s} + \mathbf{B}^{+s}\mathbf{T}_c)^{-1}\mathbf{B}^{0h}]. \quad (16)$$

Equation (16) gives the scattering T matrix of the core-shell sphere under consideration. This matrix, like $\mathbf{T}_c$, has a block diagonal form: $T_{Plm;P'l'm'} = T^{(m)}_{Pl;P'l'}\delta_{mm'}$ [11]. Moreover, $T^{(m)}_{Pl;P'l'}$ vanishes identically if the magnetic (H)/electric (E) multipoles corresponding to Pl and $P'l'$ do not have the same parity, even or odd, which means that the T matrix in a given m subspace is further reduced into two submatrices. These symmetry properties, however, do not hold in any coordinate system. If α, β, γ are the Euler angles transforming an arbitrarily chosen coordinate system into the given coordinate system in which the relative permittivity tensor of the gyrotropic core has the form of Eq. (1), the T matrix is given by

$$T_{Plm;P'l'm'} = \sum_{m''} D^{(l)}_{mm''}(\alpha,\beta,\gamma)\, T^{(m'')}_{Pl;P'l'} D^{(l')}_{m''m'}(-\gamma,-\beta,-\alpha), \quad (17)$$

where $D^{(l)}$ are the appropriate transformation matrices associated with the l irreducible representation of the $O(3)$ group [12,13].

The dimensionless scattering and extinction cross sections of the sphere under consideration, normalized to the geometric cross section, when the sphere is illuminated by a plane EM wave of wave vector $\mathbf{q}_h$ and polarization defined by the unit vector $\hat{\mathbf{e}}$, are given by [14]

$$\sigma_{sc} = \frac{1}{\pi(q_h S)^2}\sum_{Plm}\left|\sum_{P'l'm'} T_{Plm;P'l'm'}\mathbf{A}^0_{P'l'm'}(\hat{\mathbf{q}}_h)\cdot\hat{\mathbf{e}}\right|^2 \quad (18)$$

and

$$\sigma_{\text{ext}} = -\frac{1}{\pi(q_h S)^2}\,\text{Re}\sum_{Plm}[\mathbf{A}^0_{Plm}(\hat{\mathbf{q}}_h)\cdot\hat{\mathbf{e}}]^* \times \sum_{P'l'm'} T_{Plm;P'l'm'}\mathbf{A}^0_{P'l'm'}(\hat{\mathbf{q}}_h)\cdot\hat{\mathbf{e}}, \quad (19)$$

respectively, with

$$\mathbf{A}^0_{Hlm}(\hat{\mathbf{q}}_h) = \frac{4\pi i^l(-1)^{m+1}}{\sqrt{l(l+1)}}\{[\alpha_l^m \cos\theta e^{i\phi} Y_{l-m-1}(\hat{\mathbf{q}}_h) + m \sin\theta Y_{l-m}(\hat{\mathbf{q}}_h) + \alpha_l^{-m} \cos\theta e^{-i\phi} Y_{l-m+1}(\hat{\mathbf{q}}_h)]\hat{\mathbf{e}}_1 + i[\alpha_l^m e^{i\phi} Y_{l-m-1}(\hat{\mathbf{q}}_h) - \alpha_l^{-m} e^{-i\phi} Y_{l-m+1}(\hat{\mathbf{q}}_h)]\hat{\mathbf{e}}_2\} \quad (20)$$

and

$$\mathbf{A}^0_{Elm}(\hat{\mathbf{q}}_h) = \frac{4\pi i^l(-1)^{m+1}}{\sqrt{l(l+1)}}\{i[\alpha_l^m e^{i\phi} Y_{l-m-1}(\hat{\mathbf{q}}_h) - \alpha_l^{-m} e^{-i\phi} Y_{l-m+1}(\hat{\mathbf{q}}_h)]\hat{\mathbf{e}}_1 - [\alpha_l^m \cos\theta e^{i\phi} Y_{l-m-1}(\hat{\mathbf{q}}_h) + m \sin\theta Y_{l-m}(\hat{\mathbf{q}}_h) + \alpha_l^{-m} \cos\theta e^{-i\phi} Y_{l-m+1}(\hat{\mathbf{q}}_h)]\hat{\mathbf{e}}_2\}, \quad (21)$$

where $\alpha_l^m = \frac{1}{2}[(l-m)(l+m+1)]^{1/2}$; θ and ϕ denote the angular variables of $\mathbf{q}_h$ in the chosen system of spherical coordinates; and $\hat{\mathbf{e}}_1$ and $\hat{\mathbf{e}}_2$ are the polar and azimuthal unit vectors, respectively, which are perpendicular to $\mathbf{q}_h$. We note that, if $\hat{\mathbf{e}} = \hat{\mathbf{e}}_1$ or $\hat{\mathbf{e}} = \hat{\mathbf{e}}_2$, the wave is p or s linear polarized, respectively, and if $\hat{\mathbf{e}} = (\hat{\mathbf{e}}_1 + i\hat{\mathbf{e}}_2)/\sqrt{2}$ or $\hat{\mathbf{e}} = (\hat{\mathbf{e}}_1 - i\hat{\mathbf{e}}_2)/\sqrt{2}$ it is left-circular polarized (LCP) or right-circular polarized (RCP), respectively. The absorption cross section is defined by

$$\sigma_{\text{abs}} = \sigma_{\text{ext}} - \sigma_{sc}. \quad (22)$$

It is clear from Eqs. (18), (19), and (22) that, in general, the cross sections depend on the polarization and the direction of propagation of the incident plane wave. In the particular case of a spherically symmetric particle, e.g., if in our case the core is also made of a nongyrotropic (isotropic) material, the T matrix becomes diagonal: $T_{Plm;P'l'm'} = T_{Pl}\delta_{PP'}\delta_{ll'}\delta_{mm'}$, and the cross sections solely depend on the T matrix, since $\sum_m |\mathbf{A}^0_{Plm} \cdot \hat{\mathbf{e}}|^2 = 2\pi(2l+1)$.

3. RESULTS AND DISCUSSION

We first apply our full electrodynamic multipole method, which we developed in the previous section, on the specific case of hybrid magnetoplasmonic nanoparticles consisting of a spherical cobalt core coated with a concentric spherical silver shell. Such nanoparticles can be synthesized in the laboratory and are being extensively studied experimentally [6,15–18] and theoretically [19–28], since they exhibit interesting electronic, magnetic, optical, chemical, and biological properties. In our calculations, we use the actual optical and magneto-optical constants of the constituent materials, ϵ_z, ϵ_r, ϵ_κ, ϵ_s, in the spectral region that interests us here, deduced from the experiment [29–31], while $\mu_g = 1$ and $\mu_s = 1$. Moreover, we truncate the spherical-wave expansions of the EM field at $l_{\max} = 4$; thus, we obtain 48 $[= 2l_{\max}(l_{\max}+2)]$ values of q_j and associated eigenvectors $a_{Plm;j}$ from the solution of Eq. (6). This cutoff value of $l_{\max}$ is sufficient to achieve convergence of the calculated absorption cross sections to a relative accuracy better than 10^{-6} in all cases we examined.

Magnetic circular dichroism spectroscopy measures the difference between two absorption spectra acquired using light with opposite helicity in the presence of a magnetic field parallel to the incident light direction [4]. Since the wavelength of light is much longer than the size of the nanoparticles under consideration, their optical response can be described by a dipole polarizability tensor [32,33]:

$$\overleftrightarrow{\alpha} = 4\pi\epsilon_0 S^3(\overleftrightarrow{\epsilon} - \epsilon_h \overleftrightarrow{I})(\overleftrightarrow{\epsilon} + 2\epsilon_h \overleftrightarrow{I})^{-1}, \quad (23)$$

where $\overleftrightarrow{I}$ is the diagonal unit tensor and $\overleftrightarrow{\epsilon}$ an effective particle permittivity tensor, which, in the spirit of the quasi-static Maxwell–Garnett homogenization method, is obtained by the following equation [34,35]:

$$(\overleftrightarrow{\epsilon} - \epsilon_s \overleftrightarrow{I})(\overleftrightarrow{\epsilon} + 2\epsilon_s \overleftrightarrow{I})^{-1} = \left(\frac{S_c}{S}\right)^3 (\overleftrightarrow{\epsilon}_g - \epsilon_s \overleftrightarrow{I})(\overleftrightarrow{\epsilon}_g + 2\epsilon_s \overleftrightarrow{I})^{-1}. \quad (24)$$

The permittivity tensor, $\overleftrightarrow{\epsilon}_g$, given by Eq. (1), can be readily diagonalized, and its first two diagonal elements, $\epsilon_g^{(+)} = \epsilon_z(\epsilon_r + \epsilon_\kappa)$ and $\epsilon_g^{(-)} = \epsilon_z(\epsilon_r - \epsilon_\kappa)$, correspond to LCP and RCP waves, respectively, propagating along the z direction, which is taken to be along the direction of the magnetization, while the third diagonal element is ϵ_z. Therefore, in the quasi-static approximation, the corresponding diagonal elements of $\overleftrightarrow{\alpha}$, $\alpha^{(+)}$ and $\alpha^{(-)}$, provide the (normalized) absorption cross section of the core-shell particles under consideration for LCP and RCP light incident along the z direction according to scattering theory [36]:

$$\sigma_{\text{abs}}^{(\pm)} = \frac{q_h}{\pi\epsilon_0 S^2} \operatorname{Im}\alpha^{(\pm)}. \quad (25)$$

In the absence of gyrotropy, i.e., for an unmagnetized core, $\epsilon_g^{(+)} = \epsilon_g^{(-)}$ and the two circular plasmonic modes are degenerate. Within the quasi-static approach, $\epsilon^{(+)} = \epsilon^{(-)} \equiv \epsilon$ and, in the vicinity of the resonance frequency ω_0 given by the Fröhlich condition: $\operatorname{Re}\epsilon(\omega_0) + 2\epsilon_h = 0$, in the low-loss regime $\operatorname{Im}\epsilon(\omega) \ll 1$, we obtain to first-order $\sigma_{\text{abs}} \cong A/[(\omega-\omega_0)^2 + \Gamma]$, where A and Γ are positive constants. In the presence of weak gyrotropy, $\epsilon^{(\pm)} \cong \epsilon \pm \delta\epsilon$ where $\delta\epsilon$ is a small quantity, and the degeneracy of the two circular plasmonic modes is removed. To first-order approximation, $\sigma_{\text{abs}}^{(\pm)}$ have the same Lorentzian-like spectral shape, as in the absence of gyrotropy, about ω_0 shifted downward/upward by the same small amount $\delta\omega \cong \operatorname{Re}\delta\epsilon(\omega_0)/\frac{d}{d\omega}\operatorname{Re}\epsilon(\omega)|_{\omega_0}$, i.e., $\omega_0 \pm \delta\omega$, which results in a bipolar line shape for $\Delta\sigma_{\text{abs}} \equiv \sigma_{\text{abs}}^{(+)} - \sigma_{\text{abs}}^{(-)}$, as we shall see below.

Noble metals are characterized by their relatively low losses; therefore, noble metal nanoparticles support very well defined plasmonic resonances compared with ferromagnetic metals, which exhibit large losses and very broad particle plasmon resonances in the visible range. This is clearly shown in Figs. 1(a) and 1(b), which display the absorption cross sections of a silver and an unmagnetized cobalt sphere, respectively, both of radius 20 nm. It can be seen that, though the absorption spectrum of the silver nanoparticle is characterized by a strong dipole plasmonic resonance at 3.65 eV, no such resonance appears in the corresponding spectrum of the cobalt particle due to the high absorptive losses. The characteristic silver plasmon resonance also subsists in a bimetallic particle of the same size, consisting

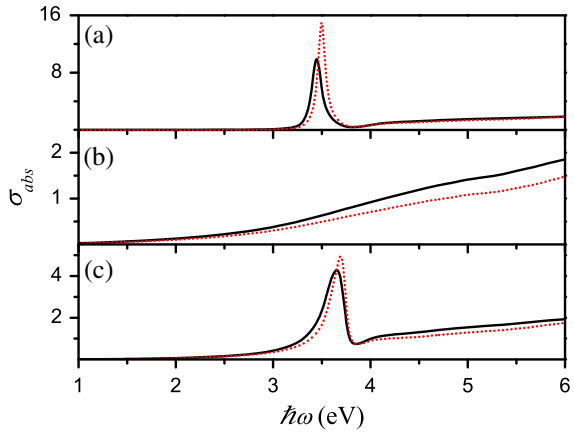

Fig. 1. (a) Calculated exact absorption cross-section spectra (solid lines) normalized to the geometric cross section of a silver sphere of radius 20 nm. (b) Unmagnetized cobalt sphere of radius 20 nm. (c) Unmagnetized cobalt sphere of radius 14 nm coated with a concentric spherical silver shell, 6 nm thick. Results of the quasi-static approximation are shown by dotted lines. In all cases, the host medium is air.

of a cobalt spherical core and a concentric spherical silver shell, as shown in Fig. 1(c). The above results agree semi-quantitatively with those of the quasi-static approximation, as can be seen in Fig. 1.

As shown in Fig. 2, with increasing the size of the cobalt core, the particle plasmon resonance shifts to higher frequencies and progressively becomes broader and less pronounced. The intensity of the associated EM field in and about the particle is overall reduced, and the field penetrates much less in the core region

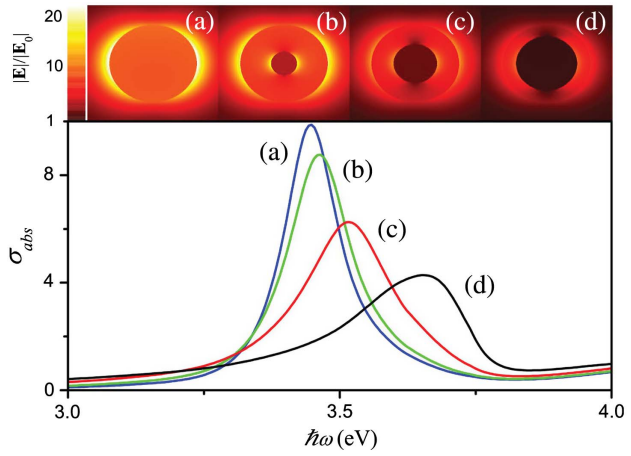

Fig. 2. (a) Calculated exact absorption cross-section spectra normalized to the geometric cross section of a silver sphere of radius 20 nm. (b) Unmagnetized cobalt sphere of radius 6 nm coated with a concentric spherical silver shell, 14 nm thick. (c) Unmagnetized cobalt sphere of radius 10 nm coated with a concentric spherical silver shell, 10 nm thick. (d) Unmagnetized cobalt sphere of radius 14 nm coated with a concentric spherical silver shell, 6 nm thick. In all cases, the host material is air. The corresponding relative (with respect to the incident plane wave) electric-field amplitude distribution in the plane of polarization, at the plasmon resonance frequency in each case, is displayed in the upper part of the figure.

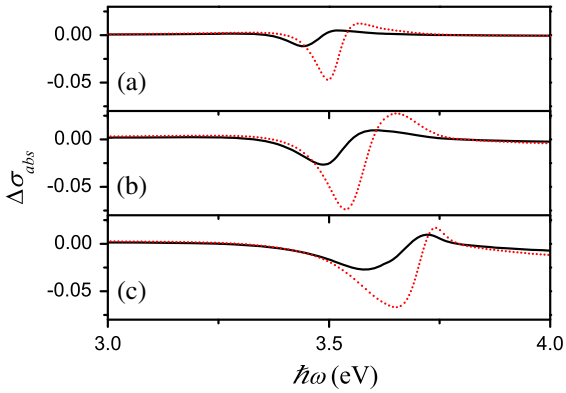

Fig. 3. Circular dichroism of core-shell cobalt-silver spheres of the same outer radius 20 nm in air. The cobalt spherical core has a radius of (a) 6 nm, (b) 10 nm, and (c) 14 nm and is magnetized along the propagation direction of the incident light. Solid lines: full electrodynamic multipole calculations. Dotted lines: quasi-static approximation.

because of the more negative real part of the permittivity of cobalt compared with that of silver at these frequencies [29,30].

We now assume that the nanoparticles under consideration are magnetized along the incident light direction, which is taken to be the z direction. We note that these particles exhibit a ferromagnetic behavior [6]. As a quantitative measure of circular dichroism, we adopt $\Delta\sigma_{\text{abs}}$, the difference between the normalized absorption cross sections for LCP and RCP incident light [37]. As previously explained, this quantity has a bipolar spectral shape that stems from the relative shift of the corresponding particle plasmon resonances due to the magneto-optic interaction. This spectral shape is indeed obtained, though with a clear asymmetry, by both full electrodynamic and quasi-static calculations, as shown in Fig. 3. The calculated relative frequency shifts between the LCP and RCP magneto-plasmonic resonances, normalized to the corresponding particle plasmon resonance frequency in the absence of gyrotropy, are of the order of 10^{-4} and vary increasingly by increasing the size of the cobalt core. We note that, in order to achieve these values with homogeneous noble metal nanoparticles, an external magnetic field as strong as 10 T is required [4]. It is also worth noting that the quasi-static approximation yields a too strong and slightly shifted in frequency circular dichroism signal. Therefore, full electrodynamic calculations are necessary for a quantitative description of the effect, even for small particles.

4. CONCLUSIONS

In summary, we extended the Mie scattering method for a core-shell sphere to the case where the core is made of a gyrotropic material. This work generalizes and complements similar recently developed methods dealing with some particular cases of the inverse morphology: A perfectly conducting sphere coated by a gyrotropic concentric spherical shell [38] or the related problem of a metallic sphere coated by a concentric spherical shell of nematic liquid crystal [39]. It is worth noting that, since our method provides, in an efficient and straightforward manner, the scattering T matrix of the single particle, it can be readily implemented into, e.g., the layer-multiple-scattering computational methodology [8,9] in order to describe the

optical properties of various structures of such hybrid gyrotropic-isotropic core-shell particles. Moreover, we applied our method to the case of core-shell cobalt-silver nanoparticles and demonstrated the occurrence of strong circular dichroism, though not to the degree predicted by the quasi-static approximation, which accounts for the necessity of the full electrodynamic treatment.

APPENDIX A

In this appendix, for the sake of completeness, we provide explicit expressions for the matrix elements of **A** [see Eq. (6)] and the $w_{lm;j}$ coefficients in Eqs. (7) and (8), which have been derived elsewhere [11]. Defining $\epsilon'_r = \epsilon_r/(\epsilon_r^2 - \epsilon_\kappa^2)$, $\epsilon'_\kappa = -\epsilon_\kappa/(\epsilon_r^2 - \epsilon_\kappa^2)$, and $\bar{\epsilon}'_r = \epsilon'_r - 1$, we have

$$A_{Hl'm';Hlm} = \frac{(l^2 + l - m^2)\epsilon'_r + m\epsilon'_\kappa + m^2}{l(l+1)}\delta_{ll'}\delta_{mm'}, \tag{A1}$$

$$A_{El'm';Hlm} = \sqrt{\frac{(l-1)(l-m)(l+m)}{(l+1)(2l-1)(2l+1)}}\frac{m\bar{\epsilon}'_r - (l+1)\epsilon'_\kappa}{l}\delta_{l-1,l'}\delta_{mm'} + \sqrt{\frac{(l+2)(l-m+1)(l+m+1)}{l(2l+1)(2l+3)}}\frac{m\bar{\epsilon}'_r + l\epsilon'_\kappa}{l+1}\delta_{l+1,l'}\delta_{mm'}, \tag{A2}$$

$$A_{Hl'm';Elm} = \sqrt{\frac{(l+1)(l-m)(l+m)}{(l-1)(2l-1)(2l+1)}}\frac{m\bar{\epsilon}'_r + (l-1)\epsilon'_\kappa}{l}\delta_{l-1,l'}\delta_{mm'} + \sqrt{\frac{l(l-m+1)(l+m+1)}{(l+2)(2l+1)(2l+3)}}\frac{m\bar{\epsilon}'_r - (l+2)\epsilon'_\kappa}{l+1}\delta_{l+1,l'}\delta_{mm'}, \tag{A3}$$

$$\begin{aligned} A_{El'm';Elm} = {} & \delta_{ll'}\delta_{mm'} + \frac{[(2l^2+2l+3)m^2 + (2l^2+2l-3)l(l+1)]\bar{\epsilon}'_r + (4l^2+4l-3)m\epsilon'_\kappa}{l(l+1)(2l-1)(2l+3)}\delta_{ll'}\delta_{mm'} \\ & - \sqrt{\frac{(l-2)(l+1)(l-m-1)(l-m)(l+m-1)(l+m)}{(l-1)l(2l-3)(2l+1)}}\frac{\bar{\epsilon}'_r}{2l-1}\delta_{l-2,l'}\delta_{mm'} \\ & - \sqrt{\frac{l(l+3)(l-m+1)(l-m+2)(l+m+1)(l+m+2)}{(l+1)(l+2)(2l+1)(2l+5)}}\frac{\bar{\epsilon}'_r}{2l+3}\delta_{l+2,l'}\delta_{mm'}, \end{aligned} \tag{A4}$$

while

$$w_{lm;j} = \sum_{l'=1}^{\infty}\sum_{m'=-l'}^{l'}(\tilde{f}_{lm}^{l'm'}a_{Hl'm';j} + \bar{f}_{lm}^{l'm'}a_{El'm';j}), \tag{A5}$$

and

$$w_{00;j} = -\sqrt{\frac{2}{3}}\epsilon'_\kappa a_{H10;j} - \sqrt{\frac{2}{15}}\bar{\epsilon}'_r a_{E20;j}, \tag{A6}$$

where

$$\tilde{f}_{l'm'}^{lm} = \sqrt{\frac{(l-m)(l+m)}{l(l+1)(2l-1)(2l+1)}}[m\bar{\epsilon}'_r - (l+1)\epsilon'_\kappa]\delta_{l-1,l'}\delta_{mm'} - \sqrt{\frac{(l-m+1)(l+m+1)}{l(l+1)(2l+1)(2l+3)}}[m\bar{\epsilon}'_r + l\epsilon'_\kappa]\delta_{l+1,l'}\delta_{mm'} \tag{A7}$$

and

$$\begin{aligned} \bar{f}_{l'm'}^{lm} = {} & \frac{(l^2+l-3m^2)\bar{\epsilon}'_r - (2l-1)(2l+3)m\epsilon'_\kappa}{\sqrt{l(l+1)}(2l-1)(2l+3)}\delta_{ll'}\delta_{mm'} - \sqrt{\frac{(l+1)(l-m-1)(l-m)(l+m-1)(l+m)}{l(2l-3)(2l+1)}}\frac{\bar{\epsilon}'_r}{2l-1}\delta_{l-2,l'}\delta_{mm'} \\ & + \sqrt{\frac{l(l-m+1)(l-m+2)(l+m+1)(l+m+2)}{(l+1)(2l+1)(2l+5)}}\frac{\bar{\epsilon}'_r}{2l+3}\delta_{l+2,l'}\delta_{mm'}. \end{aligned} \tag{A8}$$

REFERENCES

1. S. A. Maier, *Plasmonics: Fundamentals and Applications* (Springer, 2007).
2. A. Christofi and N. Stefanou, "Nonreciprocal optical response of helical periodic structures of plasma spheres in a static magnetic field," Phys. Rev. B **87**, 115125 (2013).
3. A. Christofi and N. Stefanou, "Nonreciprocal photonic surface states in periodic structures of magnetized plasma nanospheres," Phys. Rev. B **88**, 125133 (2013).
4. F. Pineider, G. Campo, V. Bonanni, C. de Julián Fernández, G. Mattei, A. Caneschi, D. Gatteschi, and C. Sangregorio, "Circular magnetoplasmonic modes in gold nanoparticles," Nano Lett. **13**, 4785–4789 (2013).
5. G. Armelles, A. Cebollada, A. García-Martín, and M. U. González, "Magnetoplasmonics: combining magnetic and plasmonic functionalities," Adv. Opt. Mater. **1**, 10–35 (2013).
6. L. Wang, C. Clavero, Z. Huba, K. J. Carroll, E. E. Carpenter, D. Gu, and R. A. Lukaszew, "Plasmonics and enhanced magneto-optics in core-shell Co-Ag nanoparticles," Nano Lett. **11**, 1237–1240 (2011).
7. Z. Lin and S. T. Chui, "Electromagnetic scattering by optically anisotropic magnetic particle," Phys. Rev. E **69**, 056614 (2004).
8. N. Stefanou, V. Yannopapas, and A. Modinos, "Heterostructures of photonic crystals: frequency bands and transmission coefficients," Comput. Phys. Commun. **113**, 49–77 (1998).
9. N. Stefanou, V. Yannopapas, and A. Modinos, "MULTEM2: a new version of the program for transmission and band-structure calculations of photonic crystals," Comput. Phys. Commun. **132**, 189–196 (2000).
10. W. C. Chew, *Waves and Fields in Inhomogeneous Media* (IEEE, 1995).
11. A. Christofi and N. Stefanou, "Layer multiple scattering calculations for nonreciprocal photonic structures," Int. J. Mod. Phys. B **28**, 1441012 (2014).
12. M. I. Mishchenko, L. D. Travis, and A. A. Lacis, *Scattering, Absorption, and Emission of Light by Small Particles* (Cambridge University, 2002).
13. T. Inui, Y. Tanabe, and Y. Onodera, *Group Theory and its Applications in Physics* (Springer, 1990).
14. G. Gantzounis and N. Stefanou, "Layer-multiple-scattering method for photonic crystals of nonspherical particles," Phys. Rev. B **73**, 035115 (2006).
15. J. Rivas, R. D. Sánchez, A. Fondado, C. Izco, A. J. García-Bastida, J. García-Otero, J. Mira, D. Baldomir, A. González, I. Lado, M. A. López-Quintela, and S. B. Oseroff, "Structural and magnetic characterization of Co particles coated with Ag," J. Appl. Phys. **76**, 6564–6566 (1994).
16. J. Rivas, A. J. García-Bastida, M. A. López-Quintela, and C. Ramos, "Magnetic properties of Co/Ag core/shell nanoparticles prepared by successive reactions in microemulsions," J. Magn. Magn. Mater. **300**, 185–191 (2006).
17. J. Garcia-Torres, E. Vallés, and E. Gómez, "Synthesis and characterization of Co@Ag core-shell nanoparticles," J. Nanopart. Res. **12**, 2189–2199 (2010).
18. J. Garcia-Torres, E. Vallés, and E. Gómez, "Measurement of the giant magnetoresistance effect in cobalt-silver magnetic nanostructures: nanoparticles," Nanotechnology **23**, 405701 (2012).
19. J. Guevara, A. M. Llois, and M. Weissmann, "Large variations in the magnetization of Co clusters induced by noble-metal coating," Phys. Rev. Lett. **81**, 5306–5309 (1998).
20. A. Dzhurakhalov, A. Rasulov, T. van Hoof, and M. Hou, "Ag-Co clusters deposition on Ag(100): an atomic scale study," Eur. Phys. J. D **31**, 53–61 (2004).
21. T. Van Hoof and M. Hou, "Structural and thermodynamic properties of Ag-Co nanoclusters," Phys. Rev. B **72**, 115434 (2005).
22. F. Dorfbauer, T. Schrefl, M. Kirschner, G. Hrkac, D. Suess, O. Ertl, and J. Fidler, "Nanostructure calculation of CoAg core-shell clusters," J. Appl. Phys. **99**, 08G706 (2006).
23. Q. Sun, A. K. Kandalam, Q. Wang, P. Jena, Y. Kawazoe, and M. Marquez, "Effect of Au coating on the magnetic and structural properties of Fe nanoclusters for use in biomedical applications: a density-functional theory study," Phys. Rev. B **73**, 134409 (2006).
24. A. A. Dzhurakhalov and M. Hou, "Equilibrium properties of binary and ternary metallic immiscible nanoclusters," Phys. Rev. B **76**, 045429 (2007).
25. T. Van Hoof, A. Dzhurakhalov, and M. Hou, "Interface formation by low energy deposition of core-shell Ag-Co nanoclusters on Ag (100)," Eur. Phys. J. D **43**, 159–163 (2007).
26. E. E. Zhurkin, T. Van Hoof, and M. Hou, "Nanoscale alloys and core-shell materials: model predictions of the nanostructure and mechanical properties," Phys. Rev. B **75**, 224102 (2007).
27. F. Dorfbauer, R. Evans, M. Kirschner, O. Chubykalo-Fesenko, R. Chantrell, and T. Schrefl, "Effects of surface anisotropy on the energy barrier in cobalt-silver core-shell nanoparticles," J. Magn. Magn. Mater. **316**, e791–e794, (2007).
28. R. Ferrando, "Symmetry breaking and morphological instabilities in core-shell metallic nanoparticles," J. Phys. Condens. Matter **27**, 013003 (2015).
29. P. B. Johnson and R. W. Christy, "Optical constants of the noble metals," Phys. Rev. B **6**, 4370–4379 (1972).
30. P. B. Johnson and R. W. Christy, "Optical constants of transition metals: Ti, V, Cr, Mn, Fe, Co, Ni, and Pd," Phys. Rev. B **9**, 5056–5070 (1974).
31. G. S. Krinchik and V. A. Artemjev, "Magneto-optic properties of nickel, iron, and cobalt," J. Appl. Phys. **39**, 1276–1278 (1968).
32. A. Lakhtakia, V. K. Varadan, and V. V. Varadan, "Low-frequency scattering by an imperfectly conducting sphere immersed in a dc magnetic field," Int. J. Infrared Millim. Waves **12**, 1253–1264 (1991).
33. A. H. Sihvola and I. V. Lindell, "Polarizability of gyrotropic sphere," Int. J. Infrared Millim. Waves **14**, 1547–1552 (1993).
34. A. H. Sihvola and O. P. M. Pekonen, "Dielectric mixtures with arbitrarily anisotropic components: focus on special gyrotropic effects," J. Electromagn. Waves Appl. **8**, 1605–1624 (1994).
35. M. Abe and T. Suwa, "Surface plasma resonance and magneto-optical enhancement in composites containing multicore-shell structured nanoparticles," Phys. Rev. B **70**, 235103 (2004).
36. C. F. Bohren and D. R. Huffman, *Absorption and Scattering of Light by Small Particles* (Wiley, 1983).
37. Z. Fan and A. O. Govorov, "Chiral nanocrystals: plasmonic spectra and circular dichroism," Nano Lett. **12**, 3283–3289 (2012).
38. Y. Song, C. M. Tse, and C. W. Qiu, "Electromagnetic scattering by a gyrotropic-coated conducting sphere illuminated from arbitrary spatial angles," IEEE Trans. Antennas Propag. **61**, 3381–3386 (2013).
39. M. Zhang and X. Zhang, "Electric field tunable photonic Hall effect with liquid crystals," Phys. Lett. A **378**, 1571–1577 (2014).